Bromination and Accompanying Rearrangement of the Polycyclic Oxetane 2,4-Oxytwistane

Murray G. Rosenberg,[‡] Peter Billing,[†] Lothar Brecker,[†] and Udo H. Brinker*[,†,‡]

[†]Department of Chemistry, Institute of Organic Chemistry, University of Vienna, Währinger Strasse 38, A-1090 Vienna, Austria
[‡]Department of Chemistry, The State University of New York at Binghamton, P.O. Box 6000, Binghamton, New York 13902-6000, United States

S *Supporting Information*

ABSTRACT: Bromination of the polycyclic oxetane 2,4-oxytwistane (rac-($1R,3S,4R,7S,9R,11S$)-2-oxatetracyclo-[5.3.1.0^{3,11}.0^{4,9}]undecane) was undertaken in order to form 2,4-dibromotwistane. The oxetane was subjected to the mild reagent combination CBr_4/Ph_3P in a fashion similar to that for the Appel and Corey–Fuchs reactions. NMR spectroscopy revealed that the isomeric dibromo compound 2,8-dibromoisotwistane (2,8-dibromotricyclo[4.3.1.0^{3,7}]decane) was inadvertently formed.

The conversion was prevented by migration of a C−C bond within the geometrically stressed C_{10} framework. Computational chemistry was used to model the structure of the polycyclic oxetane and to assess the component of total ring strain energy due to the four-membered heterocycle. Mechanistic aspects behind the skeletal rearrangement are also discussed.
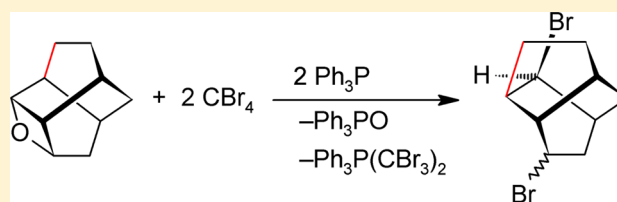
■ INTRODUCTION

Organic molecules under internal stress,[1] such as those comprising saturated ring systems whose bond angles deviate appreciably from the ideal values predicted by valence-shell electron-pair repulsion (VSEPR) theory,[2,3] can reduce the topologically derived strain energy (E_s) that results through cleavage of the weakest covalent bonds. The diminution of E_s by releasing the potential energy stored in those chemical bonds to the surroundings can be a key driving force for the exothermic reactions of such high energy compounds.[4–10] It should be noted that although these reactions are spontaneous, steep activation barriers sometimes must be overcome. Thus, reactants or reaction intermediates can resist presumably favorable bond scission due to their inherent kinetic stabilities. When this occurs, some species can tunnel quantum mechanically through the classical energy barrier or leap over it completely; photolytic elevation from the ground-state electronic potential energy surface (PES) to the excited-state electronic PES and subsequent internal conversion back to the ground state can deposit it beyond the initial barrier. In this report, an oxetane ring-opening will be explored as part of a mild bromination reaction.

Twistane (**1**; rac-($1R,3R,6R,8R$)-tricyclo[4.4.0.0^{3,8}]decane) is a tricyclic hydrocarbon that has a torsionally strained architecture featuring a C_6 twist-boat substructure embedded within it, as highlighted in Chart 1. This is not the most stable conformation for cyclohexane, unless it is positively charged,[11] because the twist-boat conformational isomer is ca. 5.5 kcal/mol higher in enthalpy ($\Delta H°$) than the more stable chair conformer.[4,12–15] Additional destabilization of the system also results, because **1** is imbued with four twist-boat faces (cf. **5** has four chair faces). 2,4-Oxytwistane (**2**; rac-($1R,3S,4R,7S,9R$,-

11S)-2-oxatetracyclo[5.3.1.0^{3,11}.0^{4,9}]undecane) is a corresponding oxetane formed by bridging C-2 and C-4 of **1** with an O atom. It is expected to be even more strained than **1** due to the presence of the extra four-membered ring (Chart 1); the E_s of oxetane alone is reported to be 25.4 kcal/mol (vide infra).[16]
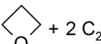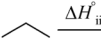
Bromination of oxetane **2** to 2,4-dibromotwistane (**6**) was the initial impetus for this study. The two C atoms bonded to the O atom of **2** (i.e., C-1 and C-3) are expected to be susceptible toward nucleophilic substitution (S_N), but only under the proper reaction conditions. In alkaline media, oxetanes are 3 orders of magnitude less reactive toward nucleophiles than are oxiranes despite being just 1.2 kcal/mol lower in E_s.[16] Thus, acid catalysis is often employed to enhance oxetane electrophilicity.[17] Common Brønsted acids, such as H_2SO_4 and HBr, have been used, and the Lewis acids BF_3,[18] $AlCl_3$,[18] and SbF_5-based[19–21] superacids are popular catalysts as well. Oxetanes are a well-known feedstock in cationic addition polymerization.[19–21] Polycyclic oxetane **2** might unravel in such a harsh environment though, so an electrophilic hypervalent non-Brønsted-acid was employed to activate the oxetane ring of **2** ultimately to attract bromide nucleophiles.[22] The nucleofugacity of an oxetane O atom is much improved when an electrophile bonds with it because the increased electron density that develops during C−O bond heterolysis can be better accommodated. Since the O atom of an oxetane is linked to two C atoms, the nucleofugal group is not a traditional leaving group, per se, until the first C−O bond is broken. The identity of that bond introduces a dichotomous situation in which the chemistry of oxetane **2** might parallel that of one of

**Chart 1. Structural Archetypes of Key Interest**

the corresponding *p*-toluenesulfonic (Ts) esters,[23,24] which undergo skeletal rearrangement during S_N1 solvolysis. Indeed, tricyclic $C_{10}H_{16}$ isomers **1**, isotwistane (**3**; (1*r*,3*S*,6*R*,7*r*)-tricyclo[4.3.1.0^{3,7}]decane), and protoadamantane (**4**; *rac*-(1*R*,3*S*,6*R*,8*R*)-tricyclo[4.3.1.0^{3,8}]decane) are intertwined in a complex web of mechanisms with adamantane (**5**; tricyclo-[3.3.1.1^{3,7}]decane) at its center.[25] It has been eloquently stated, "... that adamantane may be conceived of as a bottomless pit into which rearranging molecules may irreversibly fall."[23]

■ RESULTS AND DISCUSSION

The equilibrium geometries of oxetane **2** and oxetane (i.e., oxacyclobutane) were computed ab initio using the MP2(fc)/6-31G(d) theoretical model (Figure 1; Table 1). The most

Figure 1. Puckering angle (ϕ) of the four-membered ring and atom definitions denoted for the equilibrium geometries of (a) 2,4-oxytwistane (**2**) and (b) oxetane (optimized using the MP2(fc)/6-31G(d) theoretical model). See Table 1 for details.

Table 1. Comparative MP2(fc)/6-31G(d) Dimensions between Oxetanes[a]

measurement	oxetane 2	oxetane	difference
$r(O-C_\alpha)$ (Å)	1.467	1.452	0.015
$r(O-C_\alpha{}')$ (Å)	1.451	1.452	−0.001
$r(C_\alpha-C_\beta)$ (Å)	1.562	1.536	0.026
$r(C_\alpha{}'-C_\beta)$ (Å)	1.534	1.536	−0.002
$\theta(C_\alpha-O-C_\alpha{}')$ (deg)	87.09	91.02	−3.93
$\theta(O-C_\alpha-C_\beta)$ (deg)	89.80	92.10	−2.30
$\theta(O-C_\alpha{}'-C_\beta)$ (deg)	91.47	92.10	−0.63
$\theta(C_\alpha-C_\beta-C_\alpha{}')$ (deg)	80.97	84.78	−3.81
$\phi = 180° - abs|\omega(O-C_\alpha-C_\alpha{}'-C_\beta)|$ (deg)	33.75	0.16	33.59

[a]See Figure 1 for atom designations.

conspicuous difference is that the heterocycle is flat when free but it is puckered by ϕ = ca. 34° when embedded within the polycyclic framework of **2**. Indeed, cyclobutane is puckered similarly (ϕ = 35°).[4] Several factors determine this: (1) the height of the conformational inversion barrier, (2) angle strain,

(3) nonbonded repulsions, and (4) torsional strain.[4] Oxetane's average planarity is due to its quantum mechanically negligible inversion barrier, whereas the four-membered ring is locked into place in oxetane **2**.[26] The possible effect on ring strain energy was examined next.

One method for evaluating the strain energy of a cyclic molecule involves measuring its heat of combustion ($\Delta_{comb}H°$).[4,9] This technique was not used in this case, however, because $\Delta_{comb}H°(2)$ is unknown. In addition, the total E_s due to the separate ring components of oxetane **2** cannot be partitioned per se using the value of $\Delta_{comb}H°$ alone.[1,9,27] Thus, an estimate of the standard-state (T = 25 °C; p = 1 atm) heat of formation ($\Delta_f H°$) of oxetane **2** was sought. This can be accomplished by adding averaged enthalpies derived from hypothetical unstrained generic groups.[6,28−32] However, identifying a suitable counterpart for oxetane **2** that is devoid of an oxetane ring and calculating its $\Delta_f H°$ from group equivalents would be pointless. That is because the $\Delta_f H°$ of an oxetane (C_xH_yO) cannot be directly compared with that of a reference hydrocarbon (C_xH_{y+2}) because they have different molecular formulas. However, ring-strain energy can be approximated to a good degree of accuracy using the group equivalent method.[33] The results depend somewhat on the nature of the homodesmotic bond-separation reaction that is employed[34−36] because there is some leeway in choosing the size of the group fragments and the C atom hybridizations do not balance exactly when the molecule of concern is polycyclic (i.e., quasihomodesmotic cases).[37] The standard-state enthalpy of reaction ($\Delta H°$) is equal to $-E_s$. The value of E_s obtained for a polycyclic oxetane can then be compared with that for a reference molecule, and the difference ($\Delta\Delta H°$) can be assigned approximately to the four-membered heterocycle alone (eq 1). For oxetane **2**, E_s stems from its oxetane (Figure 1)[26] and twistane moieties. As the latter source of stress also exists in the archetypal structure **1** itself,[9] it is a suitable counterpart and a valid comparison between $E_s(2)$ and $E_s(1)$ will provide the fraction of E_s within **2** that is due to its oxetane substructure.

$$E_s(C_xH_yO)_i - E_s(C_xH_{y+2})_{ii} = \Delta H°_{ii} - \Delta H°_i = \Delta\Delta H°$$
(1)

The portion of E_s due to the oxetane ring within **2** was estimated by comparing $\Delta H°$ values for the homodesmotic[34] bond-separation reactions of oxetane **2** and reference compound **1** (eq 1, Table 2). The group equivalent method for each chemical equation was based on the simplest nearest-neighbor interactions only. The E_s of oxetane was also examined for reasons of accuracy and comparison. The $\Delta H°$ values were computed using the MP2(fc)/6-311+G(d,p)// MP2(fc)/6-31G(d) theoretical model (Table 2). The amount of E_s within **2** due to its embedded oxetane ring was calculated to be 25.3 kcal/mol (Table 2, entry a); the E_s of oxetane itself was found to be 26.2 kcal/mol (Table 2, entry b). For the sake of comparison, the theoretical method used is in general accord

Table 2. Computed Fraction (χ) of Total Ring Strain Energy (E_s) Due to Oxetane Ring[a,b]

Homodesmotic Bond-Separation Reaction	ΔH° (kcal/mol)	$\Delta\Delta H^{\circ c}$ (kcal/mol)	χ (%)
+ 12 C$_2$H$_6$ + 2 CH$_3$OH $\xrightarrow{\Delta H^\circ_i}$ (CH$_3$)$_2$O + 4 C$_3$H$_8$ + 4 (CH$_3$)$_3$CH + 2 (CH$_3$)$_2$CHOH (a-i)	−43.5	25.3	58
+ 12 C$_2$H$_6$ $\xrightarrow{\Delta H^\circ_{ii}}$ 6 C$_3$H$_8$ + 4 (CH$_3$)$_3$CH (a-ii)	−18.2[d]		
+ 2 C$_2$H$_6$ + 2 CH$_3$OH $\xrightarrow{\Delta H^\circ_i}$ (CH$_3$)$_2$O + C$_3$H$_8$ + 2 CH$_3$CH$_2$OH (b-i)	−26.2	26.2	100
$\xrightarrow{\Delta H^\circ_{ii}}$ C$_3$H$_8$ (null reaction) (b-ii)	0		

[a]Computed using the MP2(fc)/6-311+G(d,p)//MP2(fc)/6-31G(d) theoretical model. [b]Scaling factors of λ(ZPVE) = 0.9670 and $n(\Delta_{vib}H^\circ)$ = 1.0059 were used, respectively, for the ZPVE[39] and $\Delta_{vib}H^\circ$ corrections of E.[40] [c]Cf. eq 1. [d]Cf. $E_s(1)$ = 18.2 kcal/mol with reported values or those calculable from $\Delta_f H^\circ$: (1) 13.0 kcal/mol derived from $\Delta_f H^\circ_{expt}(1)$ = −21.6 kcal/mol,[41,42] (2) 21.3 kcal/mol derived from $\Delta_f H^\circ_{calc}(1)$ = −13.3 kcal/mol,[25] and (3) another computed value of $E_s(1)$ = 26.1 kcal/mol.[10]

Scheme 1. Improved Synthesis of 2-Oxatetracyclo[5.3.1.0³,¹¹.0⁴,⁹]undecane (2)[a]
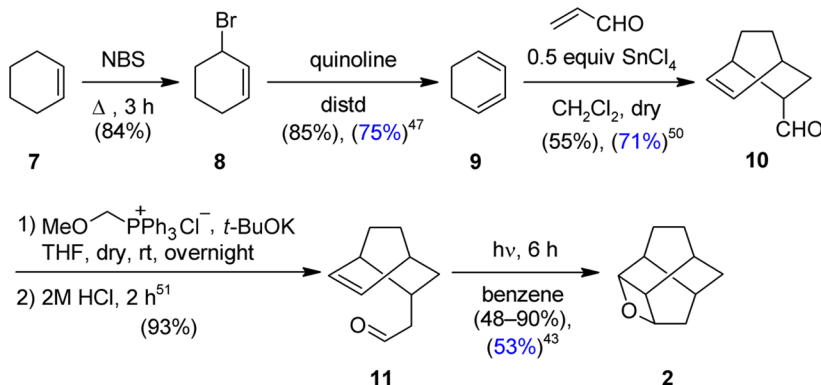
[a]Literature yields are denoted in blue.

with experimental findings. Indeed, Benson's group additivity rules advise the addition of a correction value, which is usually equal to the ring strain energy, to a compound's $\Delta_f H^\circ$ when it bears an oxetane ring: 25.2,[38] 25.7,[31] or 26.4 kcal/mol.[32,33]

The reported synthesis of oxetane **2** from *endo*-bicyclo-[2.2.2]oct-5-ene-2-carboxylic acid produces it in 19% overall yield (Scheme S1, Supporting Information),[43] but an improved method was developed herein. Oxetane **2** was synthesized from cyclohexene (**7**) in fewer steps with yields reaching 33% (Scheme 1). The five-step route began with Wohl−Ziegler bromination[44−46] of **7** followed by dehydrobromination of **8** to cyclohexa-1,3-diene (**9**).[47−49] Subsequent [4 + 2] cycloaddition with acrolein gave *endo*-bicyclo[2.2.2]oct-5-ene-2-carbaldehyde (**10**),[50] which served as the precursor for homologation (cf. Scheme S1, Supporting Information).[43] This was accomplished efficiently using a two-step, one-pot Wittig hydrolysis reaction.[51] The resulting *endo*-bicyclo[2.2.2]oct-5-en-2-ylacetaldehyde (**11**) was photolyzed with UV light to effect [2 + 2] cycloaddition of its formyl and vinylene groups (i.e., Paternò−Büchi cyclization)[52−57] to give the expected oxetane **2**.[43]

Cycloreversion of oxetane **2** may be reasonably expected. After all, the four-membered ring is responsible for more than half of the total E_s (Table 2). As mentioned, however, high energy reactants can resist ostensibly favorable bond scission(s) if they are kinetically stable. Here, two different [2 + 2] cycloreversions bisecting the oxetane ring of **2** may be envisioned (Scheme 2). A retro[2 + 2] cycloaddition from the ground state, however, is thermally forbidden according to pericyclic selection rules. Still, it should be noted that the prohibitive endothermicity of oxetane ring-opening is appreciably mitigated due to the heteroatom.[4] The formation of a stable carbonyl group from the O atom of **2** would have afforded **11**, **12**, or both (Scheme 2).

The active reagent in Appel/Corey−Fuchs reactions is triphenyl(trihalomethyl)phosphonium halide ([Ph$_3$P-(CX$_3$)]$^+$X$^−$; X = Cl, Br).[58,59] The brominating agent is formed in situ from a preequilibrated admixture of tetrabromomethane (CBr$_4$)[60] and triphenylphosphine (Ph$_3$P) (Scheme 3).[61,62] The substrates for which the Appel[63−71] and Corey−Fuchs[72−75] reaction conditions are commonly used are alcohols, oximes, aldehydes, or ketones. Cyclic ethers can also be converted into

**Scheme 2. Cycloreversion of Oxetane 2 to Aldehydes Was Not Observed**
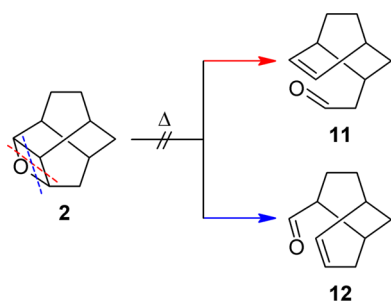
their respective α,ω-dihalo compounds in this manner.[22,76,77] For example, oxiranes react with CCl_4/Ph_3P to form *vic*-dichlorides.[76,77] An extension of this approach has been achieved using CBr_4/Ph_3P with oxetane and oxolane homologues yielding α,ω-dibromo compounds, as described in a previous report.[22] The $[Ph_3P(CBr_3)]^+Br^-$ brominating agent is milder than reagents used in traditional methods,[22,61,78] such as HBr/HOAc or PBr_3.[79−81] Oxetane **2** was thus subjected to 2 equiv of CBr_4/Ph_3P in lieu of the aforementioned reagents to avoid possible complications. Yet, despite this precaution, the target twistyl dibromo compound **6** was not produced (Scheme 4). Instead, oxetane **2** was transformed into 2,8-dibromoisotwistane (**13**; 2,8-dibromotricyclo[4.3.1.0^{3,7}]-]decane) (Scheme 4), which is an isomer of **6**. The exact mass of the unknown $C_{10}H_{14}Br_2$ compound was verified using HRMS. Its isotwistyl skeleton and positional constitution were inferred from the 2-D NMR spectra (see the Supporting Information).

Determination of the structure of dibromo compound **13** required using 1-D and 2-D NMR experiments (Figures S13–S18, Supporting Information).[82] The protons of both −CHBr− groups are conspicuously shifted downfield in the ^{1}H NMR spectrum due to their adjacent Br atoms (Figure 2). The two protons can be distinguished by their $^3J_{HH}$ couplings visible in the COSY spectrum. The signal at δ_H = 4.88 ppm is coupled to two adjacent methylidyne (>CH−) groups, while the signal at δ_H = 4.53 ppm shows coupling to a >CH− group and a methylene (−CH$_2$−) group. The former signal can only belong to the proton bound to C-2, which is the only −CHBr− group directly connected to two >CH− groups (i.e., C-1 and C-3). Next, the $^3J_{HH}$ couplings of these two >CH− groups with their vicinal groups were examined to distinguish them. One is located between two −CH$_2$− groups (i.e., C-9 and C-10) and one between a >CH− group (i.e., C-7) and a −CH$_2$− group (i.e., C-4). In the COSY spectrum, the signal at 2.72 ppm shows $^3J_{HH}$ couplings to the >CH− group at δ_H = 2.09 ppm as well as to the −CH$_2$− group with diastereotopic H atoms at δ_H = 1.79 and 2.32 ppm. Therefore, the signal at δ_H = 2.72 ppm is from H-3 and that at δ_H = 2.09 ppm arises from H-7. The latter resonance shows an additional $^3J_{HH}$ coupling to the signal at δ_H = 4.53 ppm. This scalar interaction indicates that C-7 is next to the −CHBr− group located at position 8 (Figure 2). These findings are in accord with the HMBC and NOESY spectra.

The relative configuration of C-2 with regard to that of C-8 can first be addressed by assessing the coupling constant between H-2 and H-3, which is large (i.e., $^3J_{HH}$ = 9.1 Hz). It indicates that the protons are in a *syn*- or *anti*-periplanar relationship, but the latter geometry does not exist in the isotwistyl framework. Therefore, the C-2−Br bond points toward the C-4−C-5 segment of the molecule and away from the C-8−C-9 region. The orientation of the C-8−Br bond could not be unambiguously determined (as indicated by the wavy bonds in Figure 2), however, because neither the $^3J_{HH}$ couplings nor the dipolar interactions of H-8 to either H-3 or H-6 are clearly detectable due to signal overlap at the spectrometer frequency (i.e., ν_H = 400 MHz). So, it cannot be concluded whether dibromo compound **13** is (2R^*,8R^*)- or (2R^*,8S^*)-2,8-dibromoisotwistane. In any case, the observed configuration of C-2 of **13** suggests S$_N$2-type stereospecificity. However, stereoelectronic control arising from the topology of the reaction intermediate is the more likely explanation (vide infra).

Note that 2,8-dibromoisotwistane was not the only $C_{10}H_{14}Br_2$ product isomer considered. Graph theory was applied to cast a wider net in search of rival contenders. It can be used to predict a pertinent subset of tricyclic C_{10} frameworks with four >CH− groups.[23,83] Thus, in addition to the various dibrominated forms of **1**, **3**, **4**, and **5** (cf. Chart 1), the following mathematically derived skeletal isomers of them were examined: *rac*-(1r,3r,5s,7s)-tricyclo[3.3.2.0^{3,7}]decane (**14**), 2-homotwistbrendane (**15**; *rac*-(3R,9S)-tricyclo[4.4.0.0^{3,9}]-decane), and 2-homobrendane (**16**; *rac*-(1R,4S,7S,8S)-tricyclo-[5.2.1.0^{4,8}]decane) (Chart 2). They, too, were conceptually substituted with two Br atoms to form subsets of all possible positional isomers (Table S2, Supporting Information). All compounds that did not satisfy certain requirements were rejected. First, their structures had to be consistent with the NMR evidence. Second, they had to be mechanistically feasible. The latter restriction is less rigorous because one should remain open to new chemistry. One important observation was that the product has a >CH−CHBr−CH< group and a >CH−CHBr−CH$_2$− group. Thus, some isomers could be ruled out a priori. There were some promising candidates that could have been formed in alternate mechanisms than the one presented in Scheme 8. 2,4-Dibromoisotwistane (**17**) is mechanistically feasible (Chart 3), but **17** cannot be the product because each H atom of its −CHBr− groups is positioned vicinal to a shared >CH− group at C-3. That constitution should engender $^3J_{HH}$ couplings from one >CH− signal to both −CHBr− groups' resonances, but such couplings were not exhibited in the COSY spectrum. Similarly, 2,10-dibromoprotoadamantane (**18**) was a promising candidate (Chart 3). It, too, could result from a skeletal rearrangement, but the structure of **13** cannot be that of **18**. Both of the −CHBr− groups of **18** are flanked by two >CH− groups, which is contrary to the ^{1}H NMR evidence. The same argument can be made for 2,6-dibromoadamantane (**19**) as well as 2,4-dibromoadamantane (**20**), which violates all of the tenets outlined above (Chart 3).

Scheme 3. In Situ Formation of the Appel/Corey−Fuchs Brominating Agent
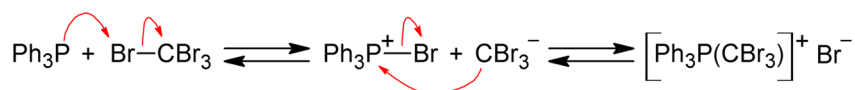
Scheme 4. Bromination of Oxetane 2 under Appel/Corey−Fuchs Reaction Conditions Led to Rearranged Dibromo Compound 13
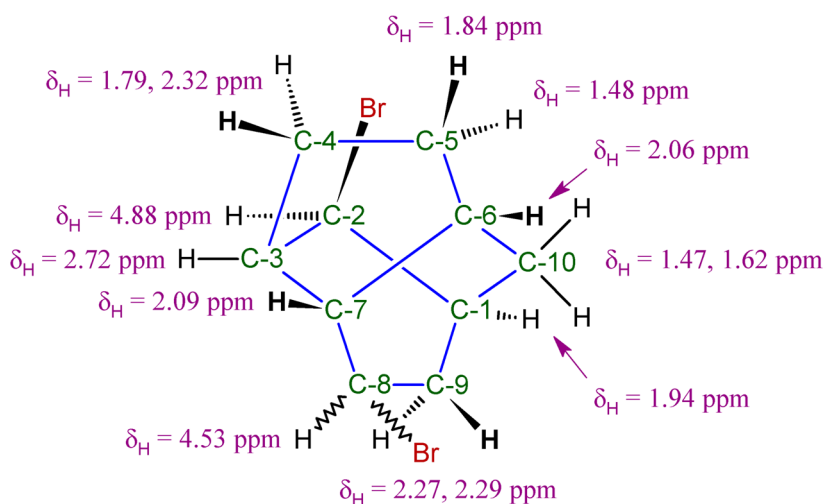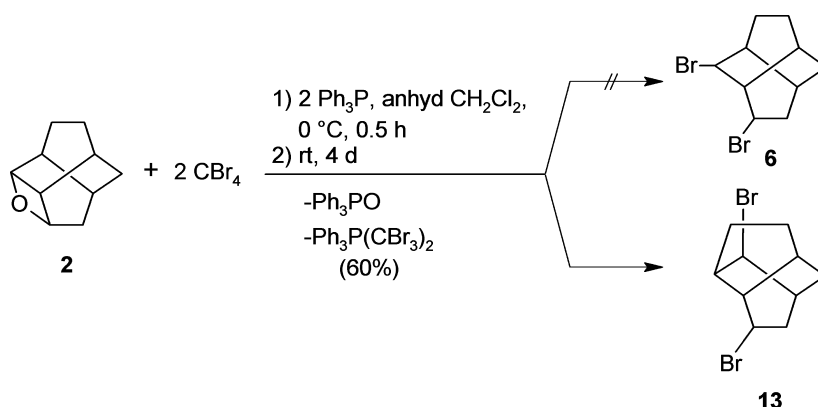
Figure 2. Structural determination of dibromo compound **13** was based in part on ^{1}H NMR resonance assignments.

Chart 2. Isomeric $C_{10}H_{16}$ Structures Derived from Graph Theory
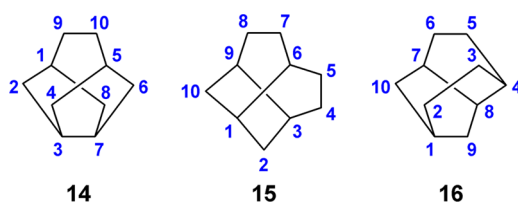
Chart 3. Rival $C_{10}H_{14}Br_2$ Candidates Dismissed on the Basis of ^{1}H NMR
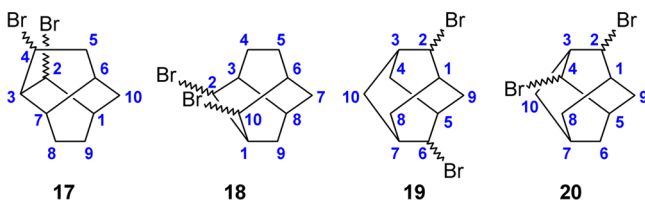
The formation of a 2-oxidotwist-4-ylium or 4-oxidotwist-2-ylium ion from oxetane **2** by two competing C−O bond heterolyses may be envisioned. The preferred generation of one isomer over the other depends on each one's E_a barrier. So, it is possible that the less stable isomer is formed faster. In any case, each reaction intermediate is prone to rapid skeletal rearrange-

ment and gives its own set of products. Oxetane **2** is thus able to reveal which of the two possible C−O heterolyses is preferred by virtue of which product (set) is formed. Separate acetolysis studies using twist-2-yl and twist-4-yl tosylates have been reported.[23,24] Acetolysis of twist-4-yl tosylate (**21**) produced an equilibrium mixture of twist-4-yl acetate (**22**) and protoadamant-10-yl acetate (**23**) and a trace amount of twist-4-ene (**24**) (Scheme 5a).[24] The agency of a pentacoordi-nate[84−96] carbocation (i.e., carbonium ion)[97] was proposed in favor of a rapidly equilibrating mixture of classical tricoordi-nate[95,98] carbocations in order to explain the skeletal rearrange-ment.[24] The C-1−O-2 bond in oxetane **2** does not break because the product, which was concluded to be **13**, possesses neither a twistyl (e.g., **6**) nor a protoadamantyl (e.g., **18**) skeleton. Solvolysis of the complementary twist-2-yl tosylate (**25**) gave six uncharacterized products, yet the following acetates were ruled out: twist-2-yl, protoadamant-2-yl, adamant-1-yl, and adamant-2-yl (**26−29**, respectively; Scheme 5b).[23] The S_N1 reaction of singly nucleofugal tosylate **25** should roughly parallel that of doubly nucleofugal oxetane **2** because the C-3−O-2 bond of oxetane **2** is the C−O bond that breaks. Since oxetane **2** is now known to give isotwistyl dibromo compound **13**, the reaction mechanisms for both **2** and **25** likely involve isotwist-2-ylium ions that stem from the irreversible rearrangements of twist-2-ylium ions.

Scheme 5. Oxetane 2 May Be Compared with a Complementary Pair of Twistyl Tosylates

(a)

(b)
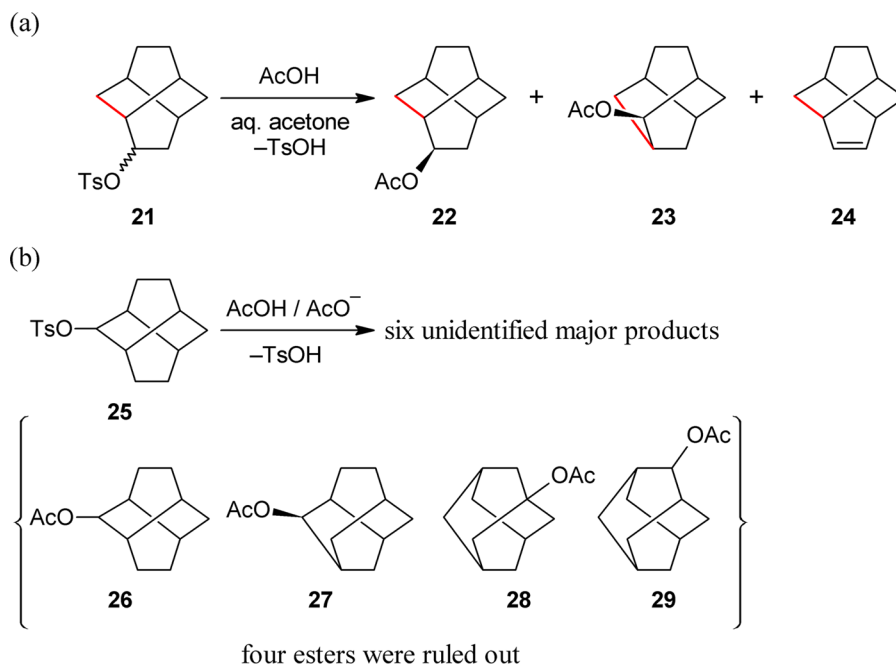
Scheme 6. Elimination Reactions of Twist-2-ylium and Twistyl-4-ylium Ions

(a)

(b)
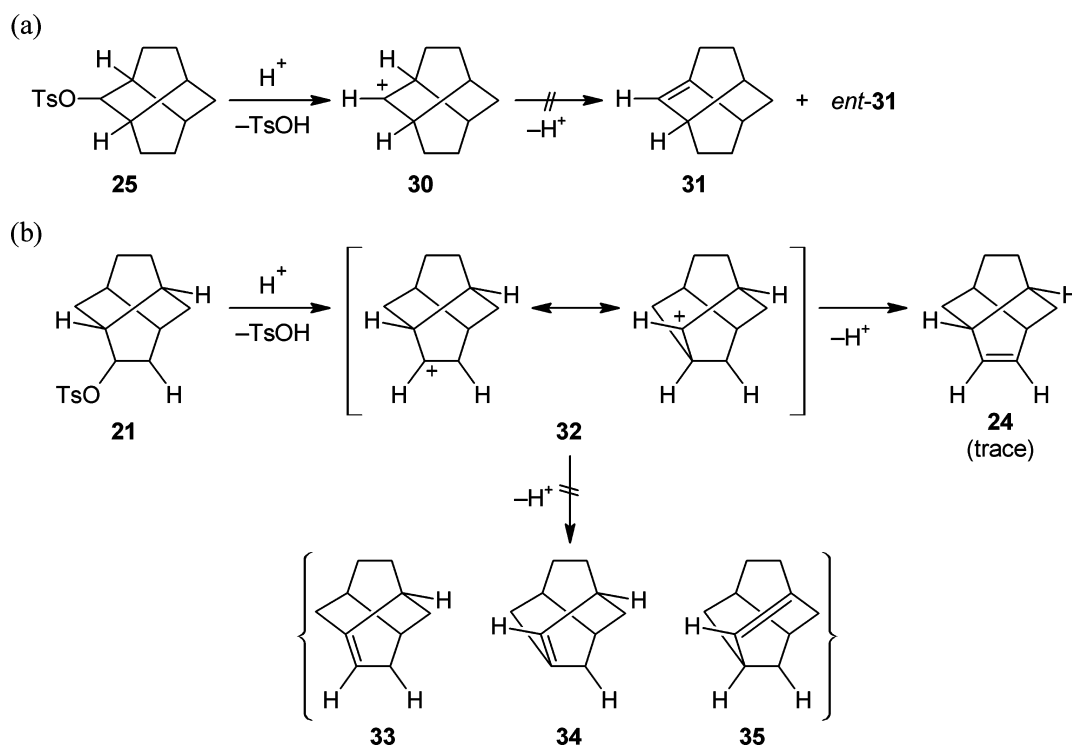
The possible diversion of carbocation intermediates from an S_N1 to an E1 pathway must be addressed. Elimination reactions of twist-2-ylium ions should be thwarted because the resulting tricycloalkene(s) would violate Bredt's rule. The bridgehead tricycloalkene twist-1-ene (**31**) is destabilized by its twisted double bond (Scheme 6a). Thus, the unsubstituted twist-2-ylium ion (**30**) cannot decay via facile E1 thereby possibly increasing its lifetime. In contrast, a trace amount of twist-4-ene (**24**) was formed during acetolysis of tosylate **21** (Schemes 5a and 6b).[24] It does not violate Bredt's rule. It is expected to derive from E1 decay of the classically tricoordinate twist-4-ylium ion (Scheme 6b), whose existence is uncertain. Computational results using a suitable theoretical model could shed light on the extent of σ-delocalization within carbonium ion **32**, which is not symmetric. The formation of other side products via E1, such as twist-3-ene (**33**), protoadamant-1(10)-ene (**34**), and protoadamant-6(10)-ene (**35**), is unlikely, because each is a bridgehead tricycloalkene that violates Bredt's rule.

The mechanism by which oxetane **2** is transformed into dibromo compound **13** will now be discussed. The in situ generation of the triphenyl(tribromomethyl)phosphonium bromide Appel/Corey–Fuchs reagent (Scheme 3) is well established,[58,59,72] but its ability to react with oxetane **2** must be explored. The pK_a of the conjugate acid of $(CH_3)_2O$ is −3.8 ($K_a = 6.3 \times 10^3$ M).[99] It is therefore a stronger Brønsted acid than the conjugate acid of 3,3-dimethyloxetane, which has a pK_a of −2.56 ($K_a = 3.63 \times 10^2$ M).[16] Thus, conversely, the conjugate base 3,3-dimethyloxetane[17] is a stronger Brønsted base than the conjugate base $(CH_3)_2O$. It should be noted, however, that the acidity of oxetanes is sensitive to their substitution pattern and the exact pK_a of oxetane **2** is not yet known.[16] More importantly, the $[Ph_3P(CBr_3)]^+$ ion is an electrophilic hypervalent non-Brønsted acid, which is the reason why it was specifically chosen for this study. Therefore, a typical neutralization reaction cannot be used to gauge the (A)cid/(B)ase interaction and another technique is needed.

The position of the equilibrium between oxetane **2** and $[Ph_3P(CBr_3)]^+Br^-$,[58,59] as shown in Scheme 7, can be approximated using the hard and soft acid and base (HSAB) principle.[100,101] The $[Ph_3P(CBr_3)]^+$ ion can act as a Lewis acid, because the virtual d-orbital of the P atom can accept a lone-pair of electrons to formally expand its octet (Scheme 7). Its (A)cid/(B)ase interaction with oxetane **2** can thus be assessed semiquantitatively by applying eqs 2–4:[100]

$$\text{hardness } (\eta) = 1/2(E_{LUMO} - E_{HOMO}) \qquad (2)$$

$$\text{absolute electronegativity } (\chi) = -1/2(E_{LUMO} + E_{HOMO}) \qquad (3)$$

(fractional) no. of electrons transferred (ΔN)

$$= 1/2\left(\frac{\chi_A - \chi_B}{\eta_A + \eta_B}\right) \qquad (4)$$

The results from three different theoretical models are presented in Table 3. Method C may yield the most likely

Table 3. Estimated (Fractional) Number of Electrons Transferred (ΔN) Initially from Oxetane 2 to the $[Ph_3P(CBr_3)]^+$ Ion (cf. Scheme 7)

method	E_{HOMO} (eV)	E_{LUMO} (eV)	$-\chi$ (eV)	η (eV)	ΔN
A[a]	−12.98	−4.23	−8.61	4.37	0.21
B[b]	−10.57	−5.82	−8.20	2.38	0.23
C[c]	−10.51	−6.96	−8.73	1.78	0.28

[a]PM7.[103] [b]B3LYP/6-311+G(d,p)//B3LYP/6-31G(d). [c]SVWN1-RPA/6-311G(d,p)//HF/3-21G(*).

value of η for two reasons: (a) the cation's geometry was optimized using a simple method and basis set that is known to accurately describe hypervalent species, and (b) the single-point energy was computed using the local spin-density approximation of DFT, which is superior to the newer *meta*-generalized gradient-approximation in this case.[102] With its low $\eta = 1.78$ eV, the polarizable $[Ph_3P(CBr_3)]^+$ ion is softer than other phosphorus-containing species (cf. Table 4).[100,101] The MP2(fc)/6-311+G(d,p)//MP2(fc)/6-31G(d) theoretical model of oxetane **2** (cf. Table 2) predicts $E_{HOMO} = -10.36$ eV and $E_{LUMO} = 1.74$ eV. Thus, $\eta(2) = 6.05$ eV and $-\chi(2) = -4.31$ eV. This is within the range of the values for $(CH_3)_2O$: $\eta = 8.0$ eV and $-\chi = -2.0$ eV.[100] Using the η and χ values of the

Table 4. Hardness (η) Parameters of Select Phosphorus-Containing Compounds

compd	η (eV)
PF_3	6.7
PH_3	6.0
$(CH_3)_3P$	5.9
PCl_3	4.7
PBr_3	4.2

(A)cid/(B)ase pair, one calculates from eq 4 that ΔN(Scheme 7) = 0.28. The low value of ΔN implies, especially since the χ-values for oxetane **2** and the $[Ph_3P(CBr_3)]^+$ ion are fairly disparate, that the forward reaction in Scheme 7 is unfavorable. Moreover, the rate of reaction between them may be hampered by steric factors despite their mutual philicities. Access to the P atom of the $[Ph_3P(CBr_3)]^+$ ion may be impeded by the four organic substituents. This may explain the long reaction time that was required (Scheme 4).

Oxetane **2** nestles within the three propeller-like phenyl groups of the $[Ph_3P(CBr_3)]^+$ ion to slowly form the cation *rac*-(1R,2S,3S,4R,7S,9R,11S)-2-[triphenyl(tribromomethyl)phosphoranyl]-2-oxoniatetracyclo[5.3.1.0^{3,11}.0^{4,9}]undecane (**36**) (Scheme 7). Concomitant ejection of the anion $(CBr_3)^-$

Scheme 7. Reversible Phosphorylation of 2,4-Oxytwistane (2) by the Appel/Corey–Fuchs Reagent
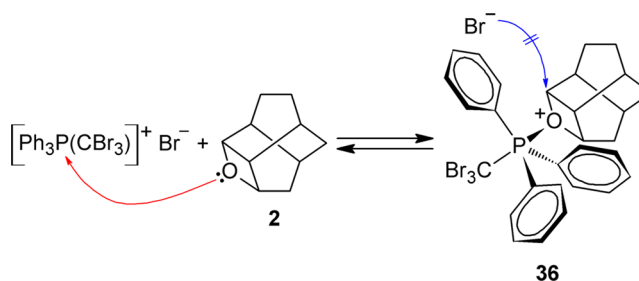
from cation **36** would produce a sterically less crowded structure, but it would create a dicationic species bearing formal positive charges on the neighboring P and O atoms. In addition, Coulombic attraction should prevent such an ionization. The fate of an oxetanium ion varies.[104] The trivial reverse reaction occurs if the forward reaction is endothermic and gives a new bond that is weak (Scheme 7).[16] This may be the case when the HSAB principle is violated.[100] The successful phosphorylation of oxetane **2**, however, is followed by a sequence of rapid events because oxetane **2** can bond more easily with electron-pair donors when it is activated. These can be nucleophilic solvents or solutes but they can also be the C–C or C–H σ-bonds that are within the reactant itself. For unsymmetric oxetanes, the ratio of regioisomeric products often indicates the molecularity of the rate-determining step.[104,105] The nonequivalent 2°-C atoms bonded to the O atom of cation **36** may be susceptible toward associative (e.g., S$_N$2), dissociative (e.g., S$_N$1), or borderline (e.g., S$_N$2/S$_N$1) C–O displacement (Scheme 8),[16,104,106] but initially they are impervious to oncoming bromide nucleophiles due to the sprawling phosphoranyl shield (Scheme 7). The 8-{[triphenyl-(tribromomethyl)phosphoranyl]oxy}isotwist-2-ylium ion (**39**) would result from complete C-3–O-2 bond rupture, and much internal stress would be relieved. However, it is possible that the species brominated first in Scheme 9 is actually carbonium

## Scheme 8. Skeletal Rearrangement Precedes Bromination
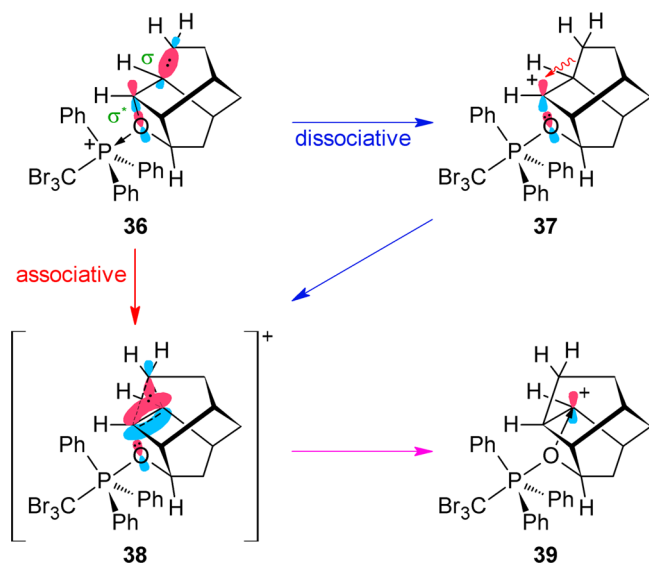
ion **38**. It profits form σ-delocalization and the relief of some internal stress (vide infra).

Unlike cation **36**, isomeric **39** is expected to undergo successful nucleophilic substitution because bromide ions do not have to contend with the bulky pendant group that continues to shield the other side of the ion. In fact, the large phosphoranyloxy group blocks the approach of bromide nucleophiles to its lobe of the virtual p-orbital on C-2 resulting in strict stereoelectronic control (cf. **39** in Scheme 9). Internal dative bonding within 8-(phosphoranyloxy)isotwist-2-ylium ion **39** may also contribute to this directing effect. The newly formed monobromo compound 2-bromo-8-{[triphenyl-(tribromomethyl)phosphoranyl]oxy]}isotwistane (**40**) was not isolated. It reacts with the second equivalent of [Ph₃P-(CBr₃)]⁺Br⁻ to yield 2,8-dibromoisotwistane (**13**) (Scheme 9). It is not clear whether the incoming bromide nucleophile dispatches the oxetane-derived phosphoranyloxy nucleofugal leaving group of **40** in an S_N2 or S_N2′ fashion, either of which would be stereospecific. The relative stereoconfiguration between C-8 and C-2 could not be determined, as explained above. Note that Scheme 9 depicts **40** → **13** as an elementary step only for the sake of simplicity. Formation of triphenyl-[bis(tribromomethyl)]phosphorane and its phosphonium ion counterpart, with which it is expected to be in equilibrium, occurs separately and is extraneous here.

The ultimate expulsion of the neutral molecule triphenyl-phosphine oxide after formation of a strong PO bond engenders a considerable driving force to the overall reaction. The opening of the four-membered ring **36** → **39** is also

expected to be exothermic, because the corresponding reduction in oxetane-derived E_s within neutral oxetane **2** is predicted to be ca. 25 kcal/mol (Table 2). The experimental and theoretical results for an uncharged oxetane ring may, however, differ for the ring's cationic form. The relief from twistyl-related stress may also factor into the formation of the isotwistyl framework of cation **39**. The $\Delta_f H°$ of isotwistane is 5.35 kcal/mol lower than that of twistane, according to molecular mechanics force-field calculations.[25,107,108] In this study, advanced correlated methods were used to compute the difference ($\Delta\Delta H°$): 5.2 kcal/mol with B3LYP/cc-pVTZ//M06-2X/6-31G(d),[109,110] 4.3 kcal/mol with EDF2/6-311+G-(d,p)//EDF2/6-31G(d),[111] 2.4 kcal/mol with M06-2X/6-311G(2df,p)//M06-2X/6-31G(d),[112] and just 1.7 kcal/mol with G3(MP2)[113] (Chart 4). The G3(MP2) thermochemical

### Chart 4. "Bottomless Pit"[23] to Adamantane[a]

Tricyclic C₁₀H₁₆ Isomer
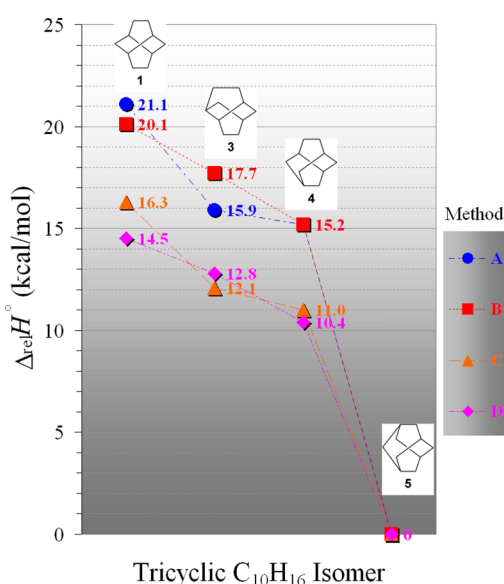
[a]The following methods were used in Chart 4: Method A: B3LYP/cc-pVTZ//M06-2X/6-31G(d); [λ(ZPVE) = 1; n(Δ_vib H°) = 1]. Method B: M06-2X/6-311G(2df,p)//M06-2X/6-31G(d); [λ(ZPVE) = 1; n(Δ_vib H°) = 1]. Method C: EDF2/6-311+G(d,p)//EDF2/6-31G(d); [λ(ZPVE) = 0.9805; n(Δ_vib H°) = 0.9947][40]. Method D: G3(MP2).

recipe also provided absolute heat of formation values for the tricyclic C₁₀H₁₆ isomers: $\Delta_f H°$(**1**) = −21.4 kcal/mol, $\Delta_f H°$(**3**) = −23.1 kcal/mol, $\Delta_f H°$(**4**) = −25.5 kcal/mol, and $\Delta_f H°$(**5**) = −35.9 kcal/mol. The $\Delta_f H°$ values for isomers **1** and **5** are in accord with experimental ones, but that for **4** is not: $\Delta_f H°$(**1**) = −21.6 kcal/mol,[41] $\Delta_f H°$(**4**) = −20.5 kcal/mol,[114−116] and $\Delta_f H°$(**5**) = −31.0 ± 1.2 kcal/mol (−30.7 kcal/mol,[117] −31.8 kcal/mol,[114−116] −32.4 kcal/mol,[117] −32.5 kcal/mol,[118] or

Scheme 9. Both Bromination Steps Happen after Oxetane 2 Has Unraveled
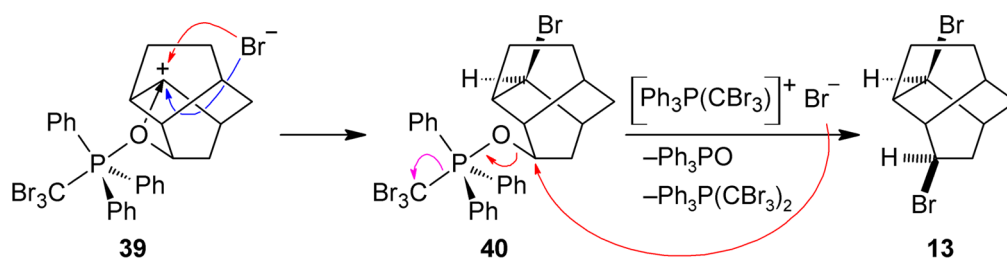
Scheme 10. S$_N$2-Type Anchimeric Assistance to Neighboring C−O Heterolysis Depends on the Dihedral Angle between the Participating Bonds
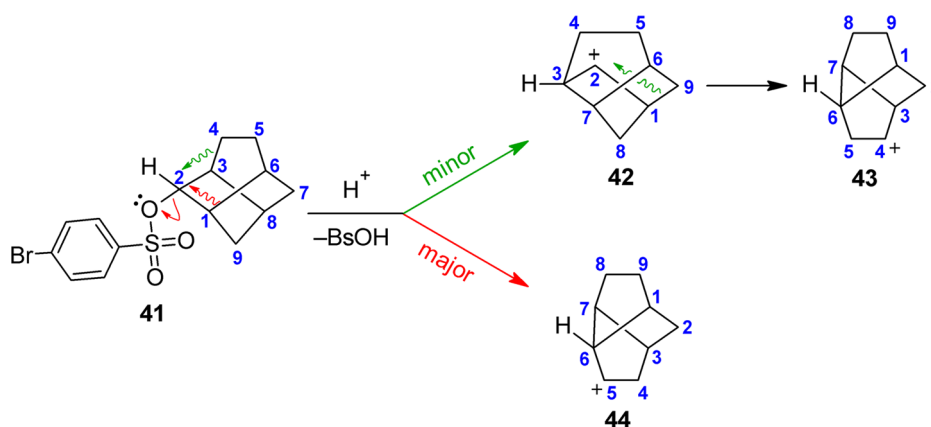
−33.0 kcal/mol[119,120]). An experimental $\Delta_f H°$ value for **3** was not found in a literature search.

Bromination of polycyclic oxetanium ion **36** is accompanied by a [1,2]-sigmatropic shift of its C-5−C-4 bond. Thus, pentacoordinate carbocation **38** (Scheme 8) necessarily comes between tricoordinate ions **37** and **39** on the intrinsic reaction coordinate. Cation **38** might be a transition state (TS) between cations **37** and **39** (i.e., **37** → [**38**]‡ → **39**) if it has more potential energy than they do. However, if it is more stable than they are then **38** may be a carbonium ion reaction intermediate that supplants them altogether:[92] [**37** ↔ **38** ↔ **39**]. As a true reaction intermediate, carbonium ion **38** would benefit energetically from the early stages of skeletal reorganization and from σ-delocalization (cf. Scheme 8). However, the modest ΔE_s (cf. eq 1; Chart 4) between isomers **1** and **3** suggests that the corresponding phosphoranyloxy carbocations **37** and **39** could be in dynamic equilibrium (e.g., **37** ⇌ [**38**]‡ ⇌ **39**; Scheme 8), wherein the structures and energies of **37** and **38** are essentially the same (cf. Hammond postulate). This interpretation is particularly attractive if internal dative bonding between the O atom and electron-deficient C atom of cation **39** exists. Such kinetic stabilization would prolong the lifetime of **39** as it is being siphoned off by surrounding bromide ions (i.e., **39** → **40**; Scheme 9).

An explanation must be given regarding the ostensible conversion of **37** to **39** (Scheme 8). Polycyclic carbocations are susceptible to Wagner−Meerwein rearrangements,[85,121,122] but one may wonder why the C-1−C-10 bond of cation **37** would migrate but the C-3−C-4 bond would not. The most plausible explanation is that **37** is not formed at all and that the conversion **36** → **39** is associative going through [**38**]‡ alone (i.e., **36** → [**38**]‡ → **39**; Scheme 8). The participation of a neighboring group, such as a C−C σ-bond electron-pair donor, can effectively enhance the rate of associative C(sp³)−O bond heterolysis if the four atoms define a 180° dihedral angle (ω). Proper molecular orbital (MO) alignment can result in anchimeric assistance that reduces the activation energy (E_a) of the elementary step **36** → **39** thereby increasing its k_{rate}. Such was observed, for example, when *exo*-twistbrend-2-yl brosylate (**41**) underwent acetolysis.[123] Skeletal rearrangement to the less stable brex-5-ylium ion (**44**) predominated because it is faster than the one leading to the more stable brend-2-ylium ion (**42**) (Scheme 10).[4,123] Cursory molecular mechanics force-field computations of **41** reveal that ω(C-4−C-3−C-2−O) = 152° whereas ω(C-6−C-1−C-2−O) = 166°,[123] which is

closer to ω_{ideal} = 180°. Therefore, the C-6−C-1 bond of **41** is better situated to assist in C−O bond heterolysis and migrate. It was postulated, based on the theory of frontier orbital overlap, that if the mechanism had been dissociative in nature, giving the corresponding twistbrend-2-ylium ion, then the C-4−C-3 bond of **41** would have been better aligned for a Wagner−Meerwein rearrangement to give cation **42**. The results of that study have bearing on this one because twistbrendane is also 4-nortwistane.[124] Presently, it is the localized C-4−C-5 σ-bond within **36** that infuses electron density into the virtual C-3−O-2 σ*-antibonding MO[122] to facilitate its heterolysis (Scheme 8). Neighboring-group participation is inevitable due to the nearly perfect *anti*-periplanarity of the C-4−C-5 and C-3−O-2 bonds (ω = 177°; Figure 1a).

It was previously noted that the three-membered oxirane ring is just 1.2 kcal/mol more strained than the four-membered oxetane ring,[16] yet the former species reacts 3 orders of magnitude more rapidly under alkaline conditions. One may therefore conclude that oxiranium ring-opening under acidic conditions should always be a fast and completely dissociative process. However, a partially associative mechanism involving transannular 1,3- and 1,5-hydride migrations appears to drive C−O heterolysis within the oxiranium ion *cis*-oxoniabicyclo-[6.1.0]nonane (**45**) (Figure 3).[125−130] The reaction is related to **36** → **39** (Scheme 8), but there are some differences: (1) it involves an oxirane, not an oxetane, (2) the strained heterocyclic ring is activated using a Brønsted acid and not an electrophilic hypervalent non-Brønsted-acid, (3) it is
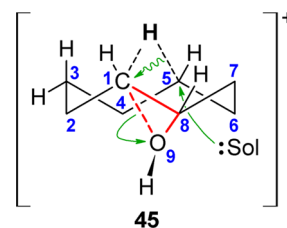

Figure 3. Oxiranium ion *cis*-oxoniabicyclo[6.1.0]nonane (**45**) undergoes transannular 1,3- and 1,5-hydride (shown here) shifts involving carbonium ions that are regio- and stereoselective due to hydride bridging. An associative 1,2-alkyl shift that accompanies C−O bond heterolysis within bridged oxetanium ion **38** may also be operating (cf. Scheme 8).

Scheme 11. Rapid Methyl Group Migration Is Likely an Associative Process[a]
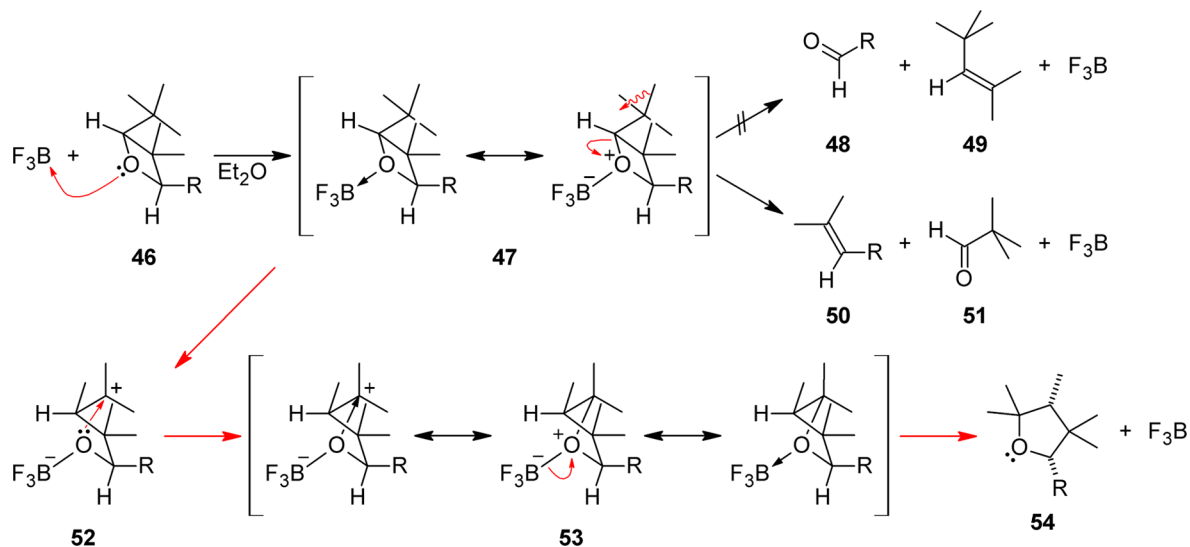
[a]R = aryl.

solvent-assisted, (4) the [1,n]-sigmatropic shift is of a hydride group, not an alkyl group, and (5) n = 3, 5 and not 2. Despite these differences, however, oxiranium ion **45** shares a similar characteristic with cationic reaction intermediate **38** (Scheme 8). They both are carbonium ions featuring two-electron, three-center bonds. Opening these small oxacycloalkane rings by C–O bond heterolysis requires backside anchimeric assistance despite the reduction in E_s that is expected to transpire.

The ring E_s of oxetane is between 25.2 and 26.4 kcal/mol (cf. Table 2, entry b; refs 31–33 and 38), yet the oxetanium ion is kinetically stable due to a 20.7 kcal/mol E_a barrier to C–O bond heterolysis.[17] Reactions of oxetanes wherein a sigmatropic rearrangement of the oxetanium ion intermediate was proposed to occur only after C–O bond heterolysis may therefore warrant further scrutiny because the C–O bond cannot fully ionize on its own sometimes. To illustrate this point, unsymmetrically substituted oxetanes that undergo nucleophilic substitution reactions without rearrangement have shown product regioselectivities indicative of borderline S_N2-/S_N1-type mechanisms.[104,105] Heterolysis of an oxetane C–O bond proceeds with assistance from well-positioned neighboring groups. Furthermore, it appears that the group's bond orbital can be so properly aligned with the C–O antibonding orbital that the group must migrate. It gets dragged from the migration origin to the migration terminus.[131]

An account involving an alkyl migration within oxetanes that were reacted under Lewis acid catalyzed conditions requires a reexamination given the new insights presented above (Scheme 11).[18] Although an oxetanium ring is presumably formed, it was not depicted in the proposed mechanism.[18] cis-2-Aryl-4-tert-butyl-3,3-dimethyloxetane (**46**) derivatives were each acidified using BF₃ (or AlCl₃).[18] With some aryl substituents, methyl group migration occurred. This was followed by intramolecular capture of the vacated C atom by the O atom ultimately yielding the ring-enlarged cis-substituted oxolanes **54** (Scheme 11). Certain aryl substituents, on the other hand, led only to retro[2 + 2] cycloaddition. The important observation was that cycloreversions to aldehydes **48** never occurred (Scheme 11). Lastly, sometimes the mechanisms competed depending on the inductive effect of the particular aryl group. The mechanistic

scheme leading to oxolanes **54** indicated that a dissociative process takes place wherein methyl group migration occurs only after C–O bond heterolysis. Since oxetane **2** and oxetanes **46** share certain structural elements, it is plausible that activated oxetanes **47** undergo an associative mechanism similar to that of oxetanium ion **36** (Scheme 8). To illustrate this, the structures in Scheme 11 are drawn to reflect the parallels. The oxetanium ions **47** possess a C–C σ-bond, within the tert-butyl group, that is anti-periplanar to the C–O σ^*-antibond. This arrangement is conducive to an associative mechanism for which ω_{ideal} = 180°. Crucially, the absence of aldehydes **48** strongly suggests that heterolysis of the C–O bond that would lead to **48** never occurs by itself. The oxetanium C–O bond is cleaved only when assisted anchimerically.

■ CONCLUSION

The bromination of oxetane **2** was accompanied by an inadvertent skeletal rearrangement of the strained C_{10} framework to dibromo compound **13** despite the mild conditions employed. The anticipated formation of dibromo compound **6** was not realized in this account. The isotwistyl skeleton and the substituent positions and configurations in **13** were confirmed by 2-D NMR spectroscopy. Dibrominated isotwistanes may be useful as starting materials in natural product syntheses.[132]

The multistep mechanism proposed for this transformation (Scheme 8) takes the following into account: (1) an organic-soluble phosphonium ion that activates oxetane **2** into cation **36**, (2) the thwarting of direct S_N2 displacement of the C–O bonds of **36** by bromide nucleophiles due to the extensive phosphoranyl pendant group, (3) the facilitation of C–O bond cleavage within **36** due to opportune anchimeric assistance from a properly aligned C–C bond within it, (4) the somewhat energetically favored skeletal rearrangement observed in the product, (5) the completely stereoselective S_N1 formation of the first C–Br bond at the newly vacated site that is farther from the still-controlling phosphoranyloxy group (Scheme 9), and (6) the possible stereospecificity for the second bromide substitution via S_N2 or S_N2' leading to the favorable departure of the neutral Ph₃PO nucleofuge and formation of dibromo compound **13**.

■ EXPERIMENTAL SECTION

Computational Methods. Quantum chemical calculations were performed using the *Spartan'14 Parallel Suite* computer program.[133] Ab initio and density functional theory (DFT) optimizations of equilibrium geometries were conducted using a 6-31G(d) basis set unless otherwise specified. Single-point energy (E) values were obtained using larger triple-ζ basis sets, as noted. Hartree−Fock wavefunctions were corrected for electron correlation either by incorporating second-order Møller−Plesset (MP2) perturbations or by using DFT methods, such as B3LYP[109,110] and M06-2X.[112] In order to convert in vacuo E values at $T = 0$ K to enthalpy ($H°$) values at $T = 298.15$ K and $p = 1.00$ atm, harmonic vibrational frequencies derived from the geometry-optimized structures were used to calculate the zero-point vibrational energy (ZPVE) and thermal vibrational energy $\Delta_{vib}H°$ values for each gas-phase molecule. The quantities were scaled by recommended factors (see Table S3, Supporting Information, for details),[40] when available, before they were added to E. The increase in kinetic energy, due to translations $(3(1/2)RT)$ and rotations $(3(1/2)RT)$, for each nonlinear molecule was also added to E. Finally, the "pV work" needed to expand one mole of ideal gas to $V = 24.466$ L (i.e., RT) was added to E (eq 5). Semiempirical computations were performed using Parametric Method 7 (PM7) as part of the *MOPAC2012* computer program.[134]

$$H° = E + \lambda \times \Delta_{ZPVE}E + n \times \Delta_{vib}H° + (3(1/2)RT)_{translational}$$
$$+ (3(1/2)RT)_{rotational} + (RT)_{ideal\,gas} \quad (5)$$

General Information. FT-NMR spectra were recorded at $T = 300$ K while applying the following radio frequencies: $\nu(^1H) = 400.13$ MHz and $\nu(^{13}C) = 100.58$ MHz. Proton and carbon-13 chemical shift (δ) values are reported relative to tetramethylsilane (TMS), although the deuterated solvents used were not doped with that internal standard. Instead, the solvents' residual peaks were used to calibrate the ^1H and ^{13}C NMR spectra: $\delta_H(CDCl_3) = 7.26$ ppm, $\delta_C(CDCl_3) = 77.16$ ppm, $\delta_H(CD_2Cl_2) = 5.30$ ppm, and $\delta_C(CD_2Cl_2) = 53.52$ ppm. Coupling constants (J) are reported in hertz. Structural assignments were made on the basis of the following 2-D NMR experiments: COSY, NOESY, HMQC, and HMBC. Accurate masses were determined by an electron-impact (EI) beam of 70 eV using a high-resolution mass spectrometer (HRMS) with a double-focusing sector field analyzer. Tandem GC−MS analyses were conducted by carrying a split sample with He gas through a 30-m poly(methylphenylsiloxane) capillary column (95% dimethyl/5% diphenyl, 0.25 mm i.d., and 0.25-μm film thickness) ending with an EI mass-selective detector (70 eV).

3-Bromocyclohex-1-ene (8). CAUTION! Five appropriately sized batches were run in parallel to control the exothermic reaction. Each one contained ca. 156 mL of cyclohexene (127 g, 1.55 mol, 5.0 equiv) and *N*-bromosuccinimide (NBS; 55 g, 0.31 mol, 1.0 equiv) in a round-bottomed flask fitted with a reflux condenser and drying tube. After 2 h of reflux, each batch was filtered to amass the filtrate into one round-bottomed flask. The residual succinimide byproduct was washed with a small amount of cyclohexene. The combined liquid was subsequently rotary-evaporated and the residual yellowish oil was purified by vacuum distillation giving 3-bromocyclohex-1-ene (209 g, 1.30 mol, 84% yield) (Figures S1 and S2, Supporting Information)[135] as a colorless oil: bp_{10} = 51 °C.

Cyclohexa-1,3-diene (9). 3-Bromocyclohexene (209 g, 1.30 mol, 1.0 equiv) and 386 mL of quinoline (422 g, 3.27 mol, 2.5 equiv) were placed into a round-bottomed flask attached with distilling equipment ending with an oil bubbler. Argon was flushed through the system to increase the final yield by 10% (Scheme 1).[47] A precipitate (likely quinolinium hydrochloride) forms if the mixture is heated too slowly. Therefore, since it eventually dissolves, the oil bath was set to maximum power to avoid precipitation. The colorless cyclohexa-1,3-diene (88.4 g, 1.10 mol, 85% yield) (Figures S3 and S4, Supporting Information)[136] liquid distilled between $T = 80$−82 °C.

***endo*-Bicyclo[2.2.2]oct-5-ene-2-carbaldehyde (10).** Cyclohexa-1,3-diene (88.4 g, 1.10 mol, 1.0 equiv) was placed into an oven-dried three-necked round-bottom flask equipped with a rubber

balloon, a low-temperature thermometer, and a pressure-equalizing dropping funnel. After the addition of 614 mL of dry CH_2Cl_2 and a small spatula tip of hydroquinone, 221 mL of acrolein (186 g, 3.32 mol, 3.0 equiv) was added at once. The flask was placed into a dry ice/acetone bath, and 71 mL of tin(IV) chloride (158 g, 0.606 mol, 0.50 equiv) dissolved in 71 mL of dry CH_2Cl_2 was added dropwise at such a rate that the inner temperature did not rise above −30 °C. Afterward, the reaction mixture was stirred overnight at about $T = -70$ °C. The reaction mixture was transferred into a separatory funnel, and 191 g of ammonium chloride was added with water until all of the solid was dissolved. The layers were separated, the aqueous layer was extracted twice with CH_2Cl_2, and the combined organic layers were washed once with brine. After drying the organic phase with sodium sulfate, the filtered solvent was rotary-evaporated and the crude product was distilled under vacuum to yield almost pure aldehyde 10 (82 g, 0.60 mol, 55%) (Figures S5 and S6, Supporting Information) as a diastereomeric mixture of *endo* and *exo* product (de = 96%, dr = 98:2): $bp_{0.1} = 28$ °C; δ_H/ppm (400.1 MHz, CDCl_3) 1.20−1.38 (2 H, m), 1.48−1.57 (1 H, m), 1.57−1.68 (2 H, m), 1.68−1.75 (1 H, m), 2.50−2.57 (1 H, m), 2.59−2.65 (1 H, m), 2.90−2.95 (1 H, m), 6.08 (1 H, ddd, ^3J 7.2, ^3J 7.3, ^4J 1.3), 6.30 (1 H, ddd, ^3J 7.2, ^3J 7.3, ^4J 1.1), 9.43 (1 H, d, ^3J 1.6), 9.7 (*exo*-10, d ^3J 0.75); δ_C/ppm (100.6 MHz, CDCl_3) 25.0, 25.4, 27.0, 29.5, 31.0, 51.2, 131, 137, 204; t_R 8.73 min (*endo*-10), 8.35 min (*exo*-10); m/z (EI) 136 (M$^+$, 10), 108 (12), 93 (8), 91 (9), 79 (100), 66 (13), 51 (8).

***endo*-Bicyclo[2.2.2]oct-5-ene-2-acetaldehyde (11).** (Methoxymethyl)triphenylphosphonium chloride (248 g, 0.724 mol, 1.20 equiv) was suspended in 945 mL of dry THF in an oven-dried three-necked round-bottomed flask equipped with a rubber balloon and a pressure-equalizing dropping funnel. Potassium *tert*-butanolate (81 g, 0.72 mol, 1.2 equiv) was added portionwise at room temperature under argon flushing, whereupon the solution turned dark red. Aldehyde 10 (82 g, 0.60 mol, 1.0 equiv) was dissolved in 300 mL of dry THF and added dropwise to the suspension within about 30 min. Then the solution was stirred overnight as the color turned to light yellow. Hydrolysis of the enol ether intermediate was achieved by adding 2 M HCl (240 mL) to the solution, which was vigorously stirred for 1.5 h. Afterward, the reaction mixture was transferred into a separatory funnel and saturated with sodium chloride, and the two phases were separated. The aqueous solution was extracted twice with Et_2O. The combined organic extracts were dried over sodium sulfate, and the filtered solvent was rotary-evaporated. The crude product was purified by vacuum distillation to yield an *endo/exo*-mixture of aldehyde 11 (84 g, 0.56 mol, 93%) as a colorless oil (de = 90%, dr = 95:5, Figures S7 and S8, Supporting Information): $bp_{0.1} = 40$ °C; δ_H/ppm (400.1 MHz, CDCl_3) 0.67−0.74 (1 H, m), 1.03−1.19 (2 H, m), 1.27−1.37 (1 H, m), 1.39−1.48 (1 H, m), 1.68−1.77 (1 H, m), 2.01−2.20 (2 H, m), 2.22−2.28 (1 H, m), 2.32−2.38 (1 H, m), 5.97 (1 H, t ^3J 7.2), 6.16 (1 H, t ^3J 7.2), 9.57 (1 H, t ^3J 1.9), 9.62 (*exo*-11, t ^3J 2.2); δ_C/ppm (100.6 MHz, CDCl_3) 24.4, 26.3, 30.0, 32.2, 34.1, 34.6, 52.2, 132, 136, 203; t_R 10.7 min; m/z (EI) 150 (M$^+$, 16), 108 (20), 91 (16), 80 (100), 65 (13).

2-Oxatetracyclo[5.3.1.0^{3,11}.0^{4,9}]undecane (2). The homologized aldehyde 11 (7.25 g, 48.3 mmol) was dissolved in 750 mL of dry benzene, and the solution was degassed by bubbling argon through it during ultrasonication. The solution was transferred into a quartz UV immersion vessel, and the photolysis was performed using a 700-W medium pressure Hg-arc lamp doped with FeI_2. Periodic monitoring by GC−MS showed that the reaction was complete after 19 h of irradiation. The polymer formed was filtered, and the filtrate was rotary-evaporated. The crude product was purified by column chromatography on 283 g of neutral aluminum oxide with EtOAc/n-C_5H_{12} 1:9 to yield oxetane 2 (trial 1: 3.48 g, 23.2 mmol, 48%. Trial 2: 6.53 g, 43.5 mmol, 90%) as small white needles (Figures S9−S11, Supporting Information): mp 118−121 °C; δ_H/ppm (400.1 MHz, CDCl_3) 1.10−1.20 (1 H, m), 1.31 (1 H, ddd J 6.3 J 6.0 J 1.7), 1.35−1.43 (2 H, m), 1.62−1.74 (4 H, m), 2.07−2.30 (3 H, m), 3.27 (1 H, "q" J 6.0), 4.28−4.34 (1 H, m), 4.62−4.67 (1 H, m); δ_C/ppm (100.6 MHz, CDCl_3) 20.6, 23.6, 25.3, 28.9, 32.5, 33.7, 39.0, 40.5, 82.8, 85.1; R_f 0.45 (EtOAc/n-C_5H_{12} = 1:9, neutral aluminum oxide); t_R 13.08

min; m/z (EI) 150 (M$^+$, 14), 132 (28), 117 (27), 104 (100), 91 (52), 79 (98), 67 (14), 53 (11); HRMS found M$^+$ 150.1043, $C_{10}H_{14}O$ requires 150.1045.

2,8-Dibromotricyclo[4.3.1.0^{3,7}]decane (13). 2,4-Oxytwistane (100 mg, 0.666 mmol, 1.0 equiv) was dissolved in 7 mL of dry CH_2Cl_2 and then CBr_4 (442 mg, 1.33 mmol, 2.0 equiv) was added to the vigorously stirred solution, which was placed into an ice bath. Triphenylphosphine (344 mg, 1.31 mmol, 2.0 equiv) dissolved in 1.4 mL of dry CH_2Cl_2 was dropped into the mixture within 30 min. The solution was then allowed to warm to room temperature and stirred for 4 days. The formed precipitate was filtered off and washed with 7 mL of Et_2O, and the combined organic solvents were rotary evaporated. The crude material was chromatographed on 7.21 g of silica gel with EtOAc/n-C_6H_{14} 5:95 (R_f = 0.5) to yield compound **13** (117 mg, 0.398 mmol, 60%) of as a colorless oil (Figures S12–S18, Supporting Information): δ_H/ppm (400.1 MHz, CDCl$_3$) 1.47 (1 H, m), 1.48 (1 H, m), 1.62 (1 H, m), 1.79 (1 H, m), 1.84 (1 H, m), 1.94 (1 H, m), 2.06 (1 H, m), 2.09 (1 H, m), 2.27 (1 H, m), 2.29 (1 H, m), 2.32 (1 H, m), 2.72 (1 H, m), 4.53 (1 H, m), 4.88 (1 H, dm J 9.1); δ_C/ppm (100.6 MHz, CDCl$_3$) 28.4, 30.3, 33.5, 35.2, 35.3, 38.9, 41.0, 47.4, 48.4, 60.5; R_f 0.44 (EtOAc/n-C_6H_{14} 5:95, silica gel); t_R 20.05 min; $\bar{v}$ /cm^{-1} (neat) 2950 (w), 1650 (w), 1010 (s), 550 (s, br); m/z (EI) 215 ([M − Br]$^+$, 72), 213 (74), 133 (91), 117 (11), 105 (27), 91 (100), 79 (36), 77 (26), 67 (14), 65 (11), 51 (8); HRMS found [M + 2]$^+$ 293.9441. $C_{10}H_{14}{}^{79}Br^{81}Br$ requires 293.9442.

■ ASSOCIATED CONTENT

Ⓢ Supporting Information

NMR and GC−MS spectra of oxetane **2** and dibromo compound **13**. NMR spectra of compounds **8−11**. Table of tricyclic $C_{10}H_{14}Br_2$ isomers derived from graph theory. Computational results of modeled compounds including Cartesian coordinates and energies. This material is available free of charge via the Internet at http://pubs.acs.org.

■ AUTHOR INFORMATION

Corresponding Author

*E-mail: udo.brinker@univie.ac.at; ubrinker@binghamton.edu.

Notes

The authors declare no competing financial interest.

■ ACKNOWLEDGMENTS

■ REFERENCES

(1) Zhao, C.-Y.; Zhang, Y.; You, X.-Z. *J. Phys. Chem. A* **1997**, *101*, 5174−5182.

(2) Bingel, W. A.; Lüttke, W. *Angew. Chem., Int. Ed. Engl.* **1981**, *20*, 899−910.

(3) Gillespie, R. J. *J. Chem. Educ.* **1963**, *40*, 295−301.

(4) Greenberg, A.; Liebman, J. F. *Strained Organic Molecules*; Academic: New York, 1978.

(5) Liebman, J. F.; Greenberg, A. *Chem. Rev.* **1976**, *76*, 311−365.

(6) Schleyer, P. v. R.; Williams, J. E.; Blanchard, K. R. *J. Am. Chem. Soc.* **1970**, *92*, 2377−2386.

(7) Wiberg, K. B. In *Reactive Intermediate Chemistry*; Moss, R. A., Platz, M. S., Jones, M., Jr., Eds.; Academic: New York, 2004; pp 714−740.

(8) Wiberg, K. B. *Angew. Chem., Int. Ed. Engl.* **1986**, *25*, 312−322.

(9) Wentrup, C. *Reactive Molecules*; Wiley: New York, 1984.

(10) Gasteiger, J.; Dammer, O. *Tetrahedron* **1978**, *34*, 2939−2945.

(11) The cyclohexyl 2°-carbocation is not isolable, but a study of the 1-methylcyclohex-1-yl 3°-carbocation showed its twist-boat conformation to be ca. 0.5 kcal/mol enthalpically more stable than the chair form. Cf. Kirchen, R. P.; Sorensen, T. S. *J. Am. Chem. Soc.* **1978**, *100*, 1487−1494.

(12) Margrave, J. L.; Frisch, M. A.; Bautista, R. G.; Clark, R. L.; Johnson, W. S. *J. Am. Chem. Soc.* **1963**, *85*, 546−548.

(13) Squillacote, M.; Sheridan, R. S.; Chapman, O. L.; Anet, F. A. L. *J. Am. Chem. Soc.* **1975**, *97*, 3244−3246.

(14) Eliel, E. L. *Angew. Chem., Int. Ed. Engl.* **1965**, *4*, 761−774.

(15) Leventis, N.; Hanna, S. B.; Sotiriou-Leventis, C. *J. Chem. Educ.* **1997**, *74*, 813−814.

(16) Searles, S. In *Comprehensive Heterocyclic Chemistry*; Katritzky, A. R.; Rees, C. W., Eds.; Pergamon: Oxford, 1984; Vol. 7, pp 363−402.

(17) Pritchard, J. G.; Long, F. A. *J. Am. Chem. Soc.* **1958**, *80*, 4162−4165.

(18) Carless, H. A. J.; Trivedi, H. S. *J. Chem. Soc., Chem. Commun.* **1979**, 382−383.

(19) Crivello, J. V. *Polym. Prepr. (Am. Chem. Soc., Div. Polym. Chem.)* **2006**, *47*, 208−209.

(20) Pruckmayr, G.; Wu, T. K. *Macromolecules* **1973**, *6*, 33−38.

(21) Rose, J. B. In *The Chemistry of Cationic Polymerization*; Plesch, P. H., Ed.; MacMillan: New York, 1963; Chapter 5.

(22) Billing, P.; Brinker, U. H. *J. Org. Chem.* **2012**, *77*, 11227−11231.

(23) Whitlock, H. W., Jr.; Siefken, M. W. *J. Am. Chem. Soc.* **1968**, *90*, 4929−4939.

(24) (a) Tichý, M.; Kniežo, L.; Hapala, J. *Collect. Czech. Chem. Commun.* **1975**, *40*, 3862−3878. (b) Tichý, M.; Kniežo, L.; Hapala, J. *Tetrahedron Lett.* **1972**, 699−702.

(25) Engler, E. M.; Farcasiu, M.; Sevin, A.; Cense, J. M.; Schleyer, P. v. R. *J. Am. Chem. Soc.* **1973**, *95*, 5769−5771.

(26) For a related account of topological compensation for the embedded oxetane ring of 2,6-oxy-7-oxabicyclo[2.2.1]heptane (ϕ = 26.9°). Cf. Pinkerton, A. A.; le Drian, C.; Vogel, P. *Acta Crystallogr.* **1996**, *C52*, 2927−2929.

(27) Dudev, T.; Lim, C. *J. Am. Chem. Soc.* **1998**, *120*, 4450−4458.

(28) Wodrich, M. D.; Schleyer, P. v. R. *Org. Lett.* **2006**, *8*, 2135−2138.

(29) Gronert, S. *J. Org. Chem.* **2006**, *71*, 1209−1219.

(30) Cohen, N.; Benson, S. W. *Chem. Rev.* **1993**, *93*, 2419−2438.

(31) *Thermochemical Kinetics: Methods for the Estimation of Thermochemical Data and Rate Parameters*, 2nd ed.; Benson, S. W., Ed.; Wiley: New York, 1976.

(32) Benson, S. W.; Cruickshank, F. R.; Golden, D. M.; Haugen, G. R.; O'Neal, H. E.; Rodgers, A. S.; Shaw, R.; Walsh, R. *Chem. Rev.* **1969**, *69*, 279−324.

(33) Bachrach, S. M. *J. Chem. Educ.* **1990**, *67*, 907−908.

(34) George, P.; Trachtman, M.; Bock, C. W.; Brett, A. M. *Tetrahedron* **1976**, *32*, 317−323.

(35) George, P.; Trachtman, M.; Brett, A. M.; Bock, C. W. *J. Chem. Soc., Perkin Trans. 2* **1977**, 1036−1047.

(36) George, P.; Trachtman, M.; Bock, C. W.; Brett, A. M. *J. Chem. Soc., Perkin Trans 2* **1976**, 1222−1227.

(37) For an authoritative treatise on the hierarchy and nomenclature of isogyric, isodesmic, hypohomodesmotic, homodesmotic, hyperhomodesmotic, and quasihomodesmotic bond-separation reactions, cf. Wheeler, S. E.; Houk, K. N.; Schleyer, P. v. R.; Allen, W. D. *J. Am. Chem. Soc.* **2009**, *131*, 2547−2560.

(38) Eigenmann, H. K.; Golden, D. M.; Benson, S. W. *J. Phys. Chem.* **1973**, *77*, 1687−1691.

(39) Csonka, G. I.; Ruzsinszky, A.; Perdew, J. P. *J. Phys. Chem. A* **2005**, *109*, 6779−6789.

(40) (a) Frequency Scale Factors for ZPVE and for $\Delta H_{vib}(T)$. Radom Group Scale Factors. http://groups.chem.usyd.edu.au/radom/More/ScaleFactor.html (accessed Jul 2, 2014). (b) Merrick, J. P.; Moran, D.; Radom, L. *J. Phys. Chem. A* **2007**, *111*, 11683−11700. (c) Scott, A. P.; Radom, L. *J. Phys. Chem.* **1996**, *100*, 16502−16513.

(41) Choi, J. K.; Joncich, M. J.; Lambert, Y.; Deslongchamps, P.; Fliszár, S. *J. Mol. Struct.* **1982**, *89*, 115−122.

(42) Fliszár, S.; Vauthier, E. C.; Chrétien, S. *J. Mol. Struct.* **2004**, *682*, 153−158.

(43) Nakazaki, M.; Naemura, K.; Nakahara, S. *J. Org. Chem.* **1978**, *43*, 4745−4750.

(44) Wohl, A. *Ber. Dtsch. Chem. Ges.* **1919**, *B52*, 51−63.

(45) Ziegler, K.; Späth, A.; Schaaf, E.; Schumann, W.; Winkelmann, E. *Justus Liebigs Ann. Chem.* **1942**, *551*, 80−119.

(46) Schmid, H.; Karrer, P. *Helv. Chim. Acta* **1946**, *29*, 573−581.

(47) Gattermann, L.; Wieland, H. *Die Praxis des organischen Chemikers*, 43rd ed.; de Gruyter: Berlin, 1982; pp 197−198.

(48) Domnin, N. A.; Larionova, M. A. *Zh. Obshch. Khim.* **1956**, *26*, 1398−1400.

(49) cf. Schaefer, J. P.; Endres, L. In *Organic Syntheses*; Baumgarten, H. E., Ed.; Wiley: New York, 1973; Collect. Vol. *5*, pp 285−288.

(50) Burnell, D. J.; Goodbrand, H. B.; Kaiser, S. M.; Valenta, Z. *Can. J. Chem.* **1987**, *65*, 154−165.

(51) Fröhlich, J.; Sauter, F.; Hametner, C.; Pfalz, M. *ARKIVOC* [Online] **2009**, 298−308. http://www.arkat-usa.org/get-file/28865/ (accessed Aug 11, 2014).

(52) D'Auria, M.; Racioppi, R. *Molecules* [Online] **2013**, *18*, 11384−11428. http://www.mdpi.com/1420-3049/18/9/11384/pdf (accessed Aug 11, 2014).

(53) Jones, G. *Org. Photochem.* **1981**, *5*, 1−122.

(54) Coyle, J. D. *Chem. Soc. Rev.* **1974**, *3*, 329−353.

(55) Coyle, J. D.; Carless, H. A. J. *Chem. Soc. Rev.* **1972**, *1*, 465−480.

(56) Pitts, J. N., Jr.; Wan, J. K. S. In *The Chemistry of the Carbonyl Group*; Patai, S., Ed.; Wiley: New York, 1966; pp 823−916.

(57) For intramolecular Paternò−Büchi cyclizations, cf. (a) Gleiter, R.; Herb, T.; Borzyk, O.; Hyla-Kryspin, I. *Liebigs Ann.* **1995**, 357−364. (b) Sauers, R. R.; Schinski, W.; Sickles, B. *Org. Photochem. Synth.* **1971**, *1*, 76.

(58) Jain, D. V. S.; Chopra, R. *Indian J. Chem.* **1982**, *A21*, 709−711.

(59) Vogt, H.; Frauendorf, C.; Fischer, A.; Jones, P. G. *Z. Naturforsch.* **1995**, *B50*, 223−228.

(60) Cao, Z.-Y. *Synlett* **2013**, *24*, 889−890.

(61) Wagner, A.; Heitz, M.-P.; Mioskowski, C. *Tetrahedron Lett.* **1989**, 557−578.

(62) Katritzky, A. R.; Nowak-Wydra, B.; Marson, C. M. *Chem. Scr.* **1987**, *27*, 477−478.

(63) Appel, R. *Angew. Chem., Int. Ed. Engl.* **1975**, *14*, 801−811.

(64) Downie, L.; Holmes, J.; Lee, J. *Chem. Ind. (London)* **1966**, *22*, 900−901.

(65) Calzada, J. G.; Hooz, J. In *Organic Syntheses*; Shinkai, I., Ed.; Wiley: New York, 1974; Vol. 54, pp 63−67.

(66) Baughman, T. W.; Sworen, J. C.; Wagener, K. B. *Tetrahedron* **2004**, *60*, 10943−10948.

(67) Newman, S. G.; Bryan, C. S.; Perez, D.; Lautens, M. *Synthesis* **2011**, 342−346.

(68) Slagle, J. D.; Huang, T. T.; Franzus, B. *J. Org. Chem.* **1981**, *46*, 3526−3530.

(69) Appel, R.; Warning, K. *Chem. Ber.* **1975**, *108*, 1437−1441.

(70) Appel, R.; Kleinstück, R.; Ziehn, K.-D. *Chem. Ber.* **1971**, *104*, 2025−2026.

(71) Lee, J. B.; Nolan, T. J. *Can. J. Chem.* **1966**, *44*, 1331−1334.

(72) Corey, E. J.; Fuchs, P. L. *Tetrahedron Lett.* **1972**, 3769−3772.

(73) Gosh, A. K.; Wang, Y. *J. Am. Chem. Soc.* **2000**, *122*, 11027−11028.

(74) Gibtner, T.; Hampel, F.; Gisselbrecht, J.-P.; Hirsch, A. *Chem.—Eur. J.* **2002**, *8*, 408−432.

(75) Mori, M.; Tonogaki, K.; Kinoshita, A. In *Organic Syntheses*; Danheiser, R. L., Ed.; Wiley: New York, 2004; Vol. 81, pp 1−13.

(76) Isaacs, N. S.; Kirkpatrick, D. *Tetrahedron Lett.* **1972**, 3869−3870.

(77) Thakore, A. N.; Pope, P.; Oehlschlager, A. C. *Tetrahedron* **1971**, *27*, 2617−2625.

(78) Arimoto, H.; Nishiyama, S.; Yamamura, S. *Tetrahedron Lett.* **1990**, 5619−5620.

(79) Cizmarikova, R.; Heger, J. *Chem. Zvesti* **1978**, *32*, 92−99.

(80) Szymanska, E.; Frydenvang, K.; Contreras-Sanz, A.; Pickering, D. S.; Frola, E.; Serafimoska, Z.; Nielsen, B.; Kastrup, J. S.; Johansen, T. N. *J. Med. Chem.* **2011**, *54*, 7289−7298.

(81) Oae, S.; Itoh, O.; Numata, T.; Yoshimura, T. *Bull. Chem. Soc. Jpn.* **1983**, *56*, 270−279.

(82) Questions may be directed to Prof. Dr. L. Brecker via E-mail: lothar.brecker@univie.ac.at.

(83) Tanaka, N.; Iizuka, T.; Kan, T. *Chem. Lett.* **1974**, 539−544.

(84) Winstein, S. In *Carbonium Ions: Major Types (Continued)*; Olah, G. A., Schleyer, P. v. R., Eds.; Wiley-Interscience: New York, 1972; Reactive Intermediates in Organic Chemistry Series; Vol. 3, Chapter 22, pp 965−1005.

(85) Story, P. R.; Clark, B. C., Jr. In *Carbonium Ions: Major Types (Continued)*; Olah, G. A.; Schleyer, P. v. R., Eds.; Wiley-Interscience: New York, 1972; Reactive Intermediates in Organic Chemistry Series; Vol. 3, Chapter 23, pp 1007−1098.

(86) Sargent, G. D. In *Carbonium Ions: Major Types (Continued)*; Olah, G. A.; Schleyer, P. v. R., Eds.; Wiley-Interscience: New York, 1972; Reactive Intermediates in Organic Chemistry Series; Vol. 3, Chapter 24, pp 1099−1200.

(87) Bartlett, P. D. *Nonclassical Carbonium Ions*; W. A. Benjamin: Menlo Park, CA, 1965.

(88) Berson, J. A. In *Molecular Rearrangements*; de Mayo, P., Ed.; Wiley-Interscience: New York, 1963; Part 1, Chapter 3, pp 111−231.

(89) Breslow, R. In *Molecular Rearrangements*; de Mayo, P., Ed.; Wiley-Interscience: New York, 1963; Part 1, Chapter 4, pp 233−294.

(90) Winstein, S.; Trifan, D. S. *J. Am. Chem. Soc.* **1949**, *71*, 2953.

(91) Olah, G. A. *Acc. Chem. Res.* **1976**, *9*, 41−52.

(92) Brown, H. C. *Acc. Chem. Res.* **1983**, *16*, 432−440.

(93) Olah, G. A.; Surya Prakash, G. K.; Saunders, M. *Acc. Chem. Res.* **1983**, *16*, 440−448.

(94) Walling, C. *Acc. Chem. Res.* **1983**, *16*, 448−454.

(95) Olah, G. A. *J. Am. Chem. Soc.* **1972**, *94*, 808−820.

(96) Rzepa, H. S.; Allan, C. S. M. *J. Chem. Educ.* **2010**, *87*, 221−228.

(97) For a synopsis of other onium compounds, cf. Tsarevsky, N. V.; Slaveykova, V.; Manev, S.; Lazarov, D. *J. Chem. Educ.* **1997**, *74*, 734−736.

(98) Traynham, J. G. *J. Chem. Educ.* **1986**, *63*, 930−933.

(99) Arnett, E. M.; Wu, C. Y. *J. Am. Chem. Soc.* **1960**, *82*, 4999−5000.

(100) Pearson, R. G. *Inorg. Chem.* **1988**, *27*, 734−740.

(101) Miessler, G. L.; Tarr, D. A. *Inorganic Chemistry*, 2nd ed.; Prentice Hall: Upper Saddle River, NJ, 1999; p 176.

(102) Hehre, W. J. *A Guide to Molecular Mechanics and Quantum Chemical Calculations*; Wavefunction Inc.: Irvine, CA, 2003; pp 130, 198, 374.

(103) Stewart, J. J. P. *J. Mol. Model.* **2013**, *19*, 1−32.

(104) Carolam, S. P. W. Ph.D. Dissertation, University of Salford, U.K., 1992, pp 25−42.

(105) Searles, S., Jr.; Pollart, K. A.; Lutz, E. F. *J. Am. Chem. Soc.* **1957**, *79*, 948−951.

(106) Tyler, D. R.; Herrick, D. R. *J. Chem. Educ.* **2002**, *79*, 1372−1376.

(107) Engler, E. M.; Androse, J. D.; Schleyer, P. v. R. *J. Am. Chem. Soc.* **1973**, *95*, 8005−8025.

(108) Ōsawa, E.; Musso, H. *Angew. Chem., Int. Ed. Engl.* **1983**, *22*, 1−12.

(109) Becke, A. D. *J. Chem. Phys.* **1993**, *98*, 5648−5652.

(110) Lee, C.; Yang, W.; Parr, R. G. *Phys. Rev. B* **1988**, *37*, 785−789.

(111) Lin, C. Y.; George, M. W.; Gill, P. M. W. *Aust. J. Chem.* **2004**, *57*, 365−370.

(112) Zhao, Y.; Truhlar, D. G. *Theor. Chem. Acc.* **2008**, *120*, 215−241.

(113) Curtiss, L. A.; Redfern, P. C.; Raghavachari, K.; Rassolov, V.; Pople, J. A. *J. Chem. Phys.* **1999**, *110*, 4703−4709.

(114) Clark, T.; Knox, T. Mc O.; McKervey, M. A.; Mackle, H.; Rooney, J. J. *J. Am. Chem. Soc.* **1979**, *101*, 2404−2410.

(115) Clark, T.; Knox, T. McO.; Mackle, H.; McKervey, M. A.; Rooney, J. J. *J. Am. Chem. Soc.* **1975**, *97*, 3835−3836.

(116) Lii, J.-H.; Allinger, N. L. *J. Mex. Chem. Soc.* **2009**, *53*, 96−107.

(117) Boyd, R. H.; Sanwal, S. N.; Shary-Tehrany, S.; McNally, D. *J. Phys. Chem.* **1971**, *75*, 1264−1271.

(118) Schulman, J. M.; Disch, R. L. *J. Am. Chem. Soc.* **1984**, *106*, 1202−1204.

(119) Bratton, W. K.; Szilard, I.; Cupas, C. A. *J. Org. Chem.* **1967**, *32*, 2019−2021.

(120) Månsson, M.; Rapport, N.; Westrum, E. F., Jr. *J. Am. Chem. Soc.* **1970**, *92*, 7296−7299.

(121) Birladeanu, L. *J. Chem. Educ.* **2000**, *77*, 858−863.

(122) Lewis, D. E. *J. Chem. Educ.* **1999**, *76*, 1718−1722.

(123) Nickon, A.; Weglein, R. C. *J. Am. Chem. Soc.* **1975**, *97*, 1271−1273.

(124) Naemura, K.; Nakazaki, M. *Bull. Chem. Soc. Jpn.* **1973**, *46*, 888−892.

(125) Cope, A. C.; Berchtold, G. A.; Peterson, P. E.; Sharman, S. H. *J. Am. Chem. Soc.* **1960**, *82*, 6366−6369.

(126) Roberts, A. A.; Anderson, C. B. *Tetrahedron Lett.* **1969**, 3883−3885.

(127) Parker, W.; Watt, C. I. F. *J. Chem. Soc., Perkin Trans. 2* **1975**, 1647−1651.

(128) McIntosh, J. M. *Can. J. Chem.* **1972**, *50*, 2152−2155.

(129) Pocker, Y. In *Molecular Rearrangements*; de Mayo, P., Ed.; Wiley-Interscience: New York, 1963; Part 1, Chapter 1, pp 1−25.

(130) Prelog, V.; Traynham, J. G. In *Molecular Rearrangements*; de Mayo, P., Ed.; Wiley-Interscience: New York, 1963; Part 1, Chapter 9, pp 593−615.

(131) A group's migratory aptitude depends mainly on three factors: (i) the intrinsic migratory aptitude, (ii) the bystander substituent at the migration origin, and (iii) the spectator substituent at the migration terminus. For reviews, cf. (a) Nickon, A. *Acc. Chem. Res.* **1993**, *26*, 84−89. (b) Merrer, D. C.; Moss, R. A. In *Advances in Carbene Chemistry*; Brinker, U. H., Ed.; Elsevier: Amsterdam, 2001; Vol. 3, pp 53−113.

(132) Biju, P. J.; Kaliappan, K.; Laxmisha, M. S.; Subba Rao, G. S. R. *J. Chem. Soc., Perkin Trans. 1* **2000**, 3714−3718.

(133) *Spartan'14 Parallel Suite, version 1.1.4*; Wavefunction Inc.: Irvine, CA, 2013.

(134) (a) *MOPAC2012, version 14.139W*; Stewart Computational Chemistry: Colorado Springs, CO, 2012. (b) Maia, J. D. C.; Urquiza Carvalho, G. A.; Mangueira, C. P.; Santana, S. R.; Cabral, L. A. F.; Rocha, G. B. *J. Chem. Theory Comput.* **2012**, *8*, 3072−3081.

(135) *NMRanalyst*, Institut für Organische Chemie, Universität Mainz (inhouse database). http://www.sciencesoft.net/3-bromocyclohexene/index.html (accessed Aug. 10, 2014).

(136) *Chemical Book*, http://www.chemicalbook.com/SpectrumEN_592-57-4_1HNMR.htm (accessed Aug 11, 2014).